Considering seafloor relief and its implications for hydrothermal exchange on Ocean Worlds

D.K. Blackman[1], N. Randolph-Flagg[2], C. Sotin[3], M Barbey[3],*
A.T. Fisher[1], A.N. Price[1], C.R. German[4]
[1]University of California Santa Cruz, USA, [2]Blue Marble Space Institute, USA
, [3]Univeristy of Nantes, France, [4]Woods Hole Oceanographic Institution, USA
**dkblackm@ucsc.edu, Earth & Planetary Sciences, UCSC, 1156 High St, Santa Cruz CA 93546 USA*

Abstract

Knowledge of the importance of seafloor relief on the distribution of hydrothermal venting into Earth's oceans motivates our exploration of how seafloor relief might develop as other Ocean Worlds evolved and whether it could persist over time scales relevant for exchange between their oceans and rocky interiors. A majority of Earth's subseafloor hydrothermal circulation occurs at low-to-moderate temperatures (≤ 100 °C) distant from active volcanic centers and driven by lithospheric (secular planetary) cooling. Similar systems could be relevant on Ocean Worlds. A brief review of Earth seafloor hydrothermal systems provides framework for consideration of basic mechanisms that could generate km-scale seafloor relief on icy moons. Simple analytic elastic flexure and viscous layer models indicate that km-scale bathymetric features could be sustained for scenarios of rocky interior properties consistent with those thought to exist on Titan and Europa, but are less likely, although not altogether ruled out, for conditions expected on Enceladus. A numerical model of Titan, with stress-dependent viscosity and spherical geometry, confirms the analytic assessment that km-scale seafloor relief could be sustained long term on other Ocean Worlds. We discuss the implications of seafloor relief for subseafloor hydrothermal flow. While observing seafloor variability on Ocean Worlds will be extremely challenging in forthcoming missions, advancing models of ocean:interior fluid exchange can benefit from awareness that seafloor relief could play an important role in the flow patterns and fluid temperatures that develop.

1. Introduction.

The discovery of oceans on several bodies in our solar system beyond Earth is driving a new phase in planetary investigation. The discovery of icy moons in which salt water oceans are in contact with silicate interiors [Nimmo & Papallardo, 2016] affords the possibility of geochemical exchange and the establishment of redox disequlibria that could be exploited by microbial metabolisms [Hand & German, 2018]. Accordingly, much current planetary research is focused on whether, and how, hydrogeologic exchange might occur on Ocean Worlds, rendering them potentially habitable [Hendrix et al., 2019, Hand et al., 2020]. Inferences about Europa's ocean chemistry based on magnetic field observations (Kivelson et al., 2004) and the composition of plume particles emitted from the ice surface of Enceladus (Hsu et al., 2015; Postberg et al, 2008; Waite et al., 2017) have been interpreted to reflect geologically recent or ongoing seawater interaction with silicates of the rocky interior (RI). Recent studies have modeled hydrothermal circulation in the RI of ocean worlds (OW) at a global scale to assess what forms of subseafloor hydrothermal circulation and associated advective heat transfer are possible (e.g., Choblet et al., 2017, Travis et al., 2012). These are important results as they indicate a plausible basis for advective and reactive processes, but experience exploring Earth's seafloor hydrothermal systems shows that local to regional variations in properties and morphology influence associated flows and related processes (Haymon et al., 1991; Humphris et al., 1995; Davis et al., 1992; Hutnak et al., 2006; Le Gal et al., 2018). Heterogeneity is the rule rather than the exception in geologic systems on Earth, at scales ranging from mm to thousands of km. Here we explore whether topographic variability on OW seafloors (bathymetry) could develop and persist at relevant spatial and temporal scales. Because we find that the occurrence of seafloor relief is physically plausible and persistence cannot be ruled out, we consider how it might influence patterns of subseafloor circulation, as has been shown to occur on Earth.

The aim of this paper is to provide information that can guide ongoing efforts to model hydrothermal flow, and associated heat transfer, on OW. This introduction contains a brief review of knowledge gathered over half a century of exploration of our own ocean floor, which illustrates how fundamental its variability can be in determining the nature of subseafloor fluid circulation. Subsequent sections consider the generation and possible scales of relief on Ocean Worlds such as Titan, Europa, and Enceladus. We test whether expected mechanical properties of the RI of ocean worlds could result in preservation of bathymetric relief over long time scales. We compare conditions on Earth to these three OWs, which serve to illustrate ranges of bathymetric relief that might be sustained on small, moderate or large OW. Both Europa and Enceladus have previously been interpreted to have recently active hydrothermal interaction between their ocean and RI. Finally, we discuss the implications of the concept of km-scale seafloor relief in terms of whether/how it might affect hydrothermal systems on an OW.

Hydrothermal circulation of seawater within Earth's ocean crust is well documented (Baker et al., 1991; German and Seyfried, 2014; Humphris et al., 1995) and thought to extract 8-10 TW of planetary heat, comprising 20-25% of Earth's global heat loss (e.g., Elderfield and Schultz, 1996; Hasterok, 2013; Mottl, 2003; Sclater et al., 1980). This advective (hydrogeologic) component of Earth's heat budget occurs across a wide range of temperatures, from barely warmer than bottom water (typically ~1-3 °C in the deep ocean) up to ~400°C at some active volcanic centers (German et al., 2023). While high temperature “black smoker” venting at mid-ocean ridges may be visually spectacular, most of Earth's advective heat loss through the seafloor occurs during low-temperature circulation (<30°C, Elderfield and Schultz, 1996; Johnson and Pruis,2003; Wheat et al., 2004) far from active seafloor spreading.

Several factors influencing subseafloor hydrothermal circulation on Earth are potentially relevant on other ocean worlds, including the distributions of planetary heat loss and bathymetric relief. Most of Earth's seafloor is far from the direct magmatic influence of active seafloor creation or mid-plate volcanism. In these 'ridge-flank' regions, the primary heat source that drives seafloor hydrothermal circulation is lithospheric cooling, the upward conduction of heat from the solid Earth and into the overlying ocean, with a global mean seafloor value of ~100 mW/m^2 (Davies and Davies, 2010; Hasterok, 2013). However, measured heat flux values on ridge flanks (which record conductive heat loss through sediments above the igneous crust) are often lower than predicted by lithospheric cooling curves, particularly on seafloor younger than ~60 M.y. This is a primary expression of advective heat extraction, which is typically not measured directly.

Bathymetry may play multiple roles in driving and guiding hydrothermal circulation and associated heat extraction from the rocky interior of OWs, as on Earth. First, bathymetric relief along a largely-isothermal, deep seafloor results in conductive refraction that causes lateral variability in heat flow into the ocean (e.g., Lachenbruch, 1968; Fisher and Harris, 2010). Isotherms in the crust tend to be more widely spaced below bathymetric highs and more closely spaced below adjacent bathymetric lows, resulting in lower and higher heat flux, respectively. Second, bathymetric relief can be associated with variations in the permeability of underlying rocks, enabling and enhancing local hydrothermal circulation. For example, volcanic features often have greater permeability due to thermal contraction of the rock cooled by seawater and a significant fraction of talus formed by local slope failures. Faults associated with deformation of the crust can also have higher permeability associated with fracture porosity and are known to channel hydrothermal flow (e.g., Clague et al., 2020; deMartin et al., 2007; Haymon et al., 1991; Tontoni et al., 2016). Finally, bathymetric relief combined with sedimentation can result in lateral variability in hydrogeologic connectivity between the crustal "aquifer" and the overlying ocean, because deep sea sediments tend to be orders of magnitude less permeable than underlying basement (e.g. Spinelli et al., 2004). Marine sediments generally collect and are thicker in bathymetric lows, amplifying the lateral differences in crust-ocean connectivity. In some cases, elevated basaltic crust that is surrounded by relatively thick and continuous sediments can develop into sites of thermally significant, outcrop-to-outcrop, fluid and heat flow (a ridge-flank "hydrothermal siphon"). Cool bottom water flows into one basement outcrop, is transported laterally, then discharges through another outcrop. This process has been documented to occur across lateral scales extending ≥ 10's of km (e.g., Fisher et al., 2003; Hutnak et al., 2008; Villinger et al., 2002; Anderson et al., 2012), with outflow temperatures controlled by the permeability and thickness of the basement aquifer, and the transmittance of inflow and outflow sites (Lauer et al., 2018; Winslow and Fisher, 2015). Ridge-flank hydrothermal siphons develop as a consequence of feedbacks between the flow rates, depths, and residence times of hydrothermal fluids. In general, larger rates of inflow, outflow and lateral flow result in lower crustal temperatures but higher rates of advective heat extraction. Having a hydrogeologic restriction at the outflow end of a hydrothermal circulation path ("discharge domination," as defined by Cann and Strens, 1989) helps to raise discharge temperature.

Typical bathymetric relief on Earth is generated by tectonic forces and volcanism, with local heights ranging 0.1-3 km and km-scale wavelength (Goff et al., 2004; Smith and Jordan, 1988). This ubiquitous seafloor relief belies more dramatic features several 10's km wide that result from basin-scale mantle convection or deformation associated with plate subduction, such as the 11 km deep Marianas Trench or the 10 km high Hawaiian Islands. Bathymetric features that are associated with seafloor hydrothermal circulation on Earth vary in amplitude from tens of meters to several kilometers, and in wavelength from a few to several tens of kilometers (Figure 1). Under the conditions of Earth's gravitational force and in-situ properties of the lithosphere, km-scale seafloor features can persist throughout the life of an oceanic plate, tens to a few hundred M.y.

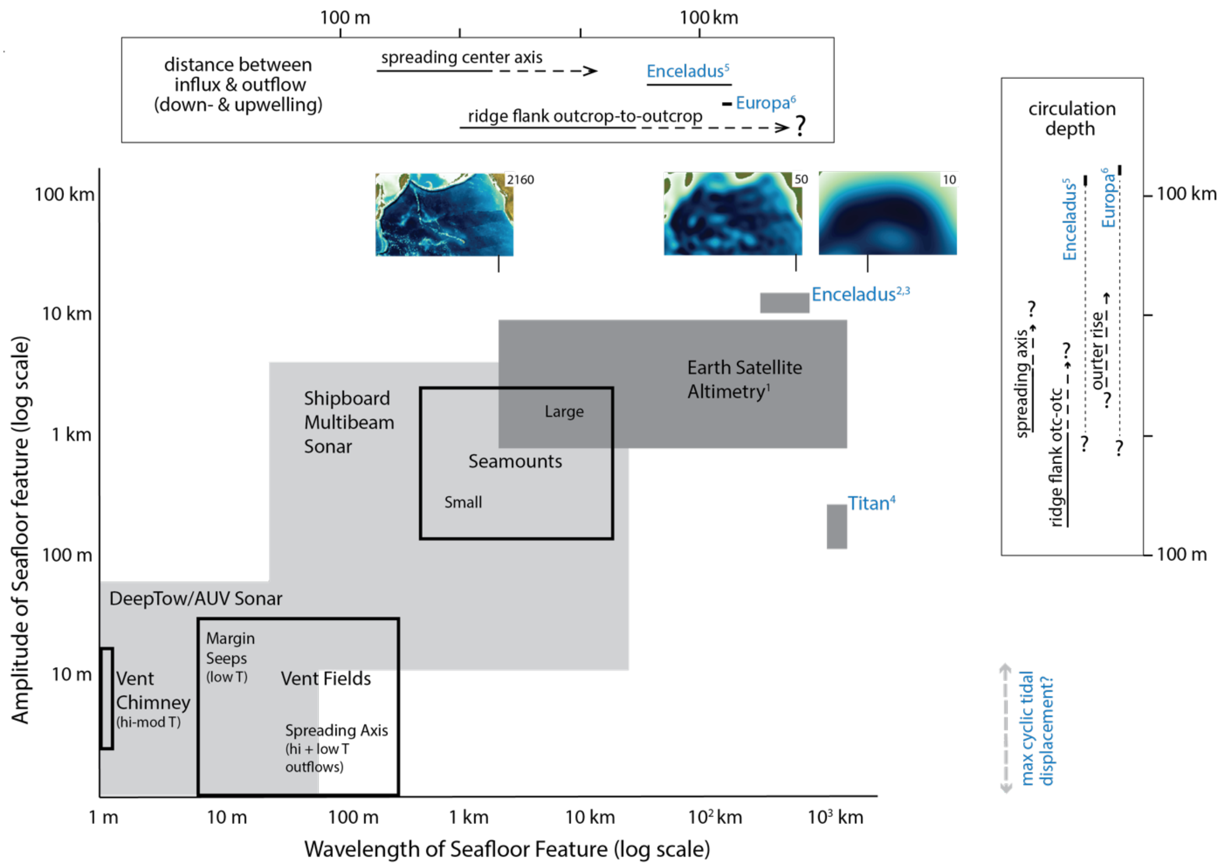

Figure 1. Spatial scales of bathymetric features that host sub-seafloor hydrothermal systems on Earth (black outlined boxes), and current data resolution for Earth and OW, for various measurement tools (shaded boxes): satellite data (dark gray); marine sonar data (light gray). T: temperature, low < 80°C; AUV: autonomous underwater vehicle. [1]Sandwell et al., 2014; [2]McKinnon, 2013; [3]Hemingway and Mittal, 2019; [4]Cadek et al., 2021. Color images show Pacific seafloor relief at 3 different spherical harmonic representations (labeled in upper right corner), with tic mark plotted at the corresponding minimum resolved wavelength of the satellite altimetry model (modified from Salaree and Okal, 2020). Boxed lateral/vertical length scales outside main plot indicate size/depth of subseafloor circulation: estimated by global OW thermal/flow models where depth of circulation is assumed (blue lettering, [5]Choblet et al., 2017; [6]Travis et al., 2012); inferred from Earth observations (black lettering) of micro-seismicity patterns (Tolstoy et al., 2008), vent fluid temperature, chemistry and chimney distributions (Delaney et al., 1997; Haymon et al., 1991), seismic imaging/anisotropy (Carbotte et al., 2012; Dunn and Forsyth, 2003; Miller et al., 2020), and numerical modeling (Lauer et al, 2018; Winslow et al., 2015; 2016).

The resolution of geophysical data that are currently available for Enceladus and Europa (spherical harmonic degree/order 2-3) are much too coarse to resolve km-scale bathymetric relief (e.g. Koh et al., 2022). Previous studies have considered a non-spherical rocky interior on Enceladus (McKinnon, 2013; Showman et al., 2013). However, the several-km radius variation of the RI that these authors determine extends over hemispheric distance. Hemingway and Mittal (2019) consider cases where RI shape would help to explain gravity and libration data, along with solved-for ice shell and ocean structures, finding that variation in bathymetry of the order 0.1-1 km could exist at wavelengths of ~500 km. Titan is thought to have bathymetric variation of 100's m amplitude and ~2500 km wavelength (degree 5) based on a similar approach (Cadek et al., 2021). For comparison, the latest satellite gravity data for Earth resolve the field to SH degree/order 2160 and, when combined with ship track sonar data/trends, reveal bathymetric features ≥ 2-3 km across (Figure 1; Sandwell et al., 2014). This resolution is sufficient to map locations of seafloor spreading centers and relatively large seamounts but does not resolve a much larger population of smaller seamounts (Kim and Wessel, 2011), some of which are known sites of hydrothermal discharge (e.g., Baby Bare and Dorado outcrops in the NE Pacific, Mottl et al., 1989; Wheat and Fisher 2008). Thus, the current and foreseeable future resolution of OW seafloor maps are sufficient to resolve modest amplitude variations, commensurate with Earth features such as abyssal hills and intermediate-to-large seamounts, but only if they have wavelengths of hundreds to thousands of kilometers.

The absence of evidence for smaller-scale bathymetric relief on OWs, due to the lack of current observational resolution, is not proof that these features do not exist. Therefore, we consider whether there are plausible mechanisms to generate km-scale bathymetric relief on OWs and assess whether such features could be supported over geologic time, given hypothesized material properties and generally low gravity of these bodies. Calculations are based on idealized geometries and a range of material properties inferred for OW interiors (e.g., Schubert et al., 2004; Hussman et al., 2015), allowing us to assess the basic possibility.

2. Processes that could generate bathymetric relief on OW

In general, seafloor relief on an Ocean World could be generated by volcanic activity, faulting, or large meteor impacts. While these processes may not be important on present-day Titan, Europa, or Enceladus, one or more of them likely occurred during their evolution. Tidal forcing could also contribute to vertical fault displacement, particularly if the subseafloor is heterogenous. We explore each of these concepts briefly below and note that if the rigidity of the seafloor is sufficient to support local bathymetric loads, any relief generated could persist over time.

Thermal models suggest that Europa likely experienced partial melting of its silicate mantle (Sotin et al., 2009) and recent work indicates convection could have occurred as well (Béhounkova et al., 2021). Partial melting in the upwelling zones could have resulted in seafloor volcanism, mostly in the distant past, and Behounkova et al. (2021) show that under occasional eccentricity conditions, tidal dissipation in the RI could lead to more recent pulses of partial melting of the silicate mantle. These authors estimate the amount of past (first ~Gyr) magma generation to be comparable to the volume that formed large igneous provinces on Earth, so it's possible that km-scale topography characterizes portions of Europa's seafloor if this melt migrated to the surface and erupted at distinct volcanic centers. Initial work by Green et al. (2023) questions whether recent partial melt could rise through Europa's lithosphere but systematic analysis confirming this result has not been reported to date.

While Titan is large enough to accumulate heat from accretion and radioactive decay, and to have experienced significant tidal dissipation in its early development (Sotin et al., 2021) temperatures achieved are believed to have been insufficient to results in silicate melting and magmatism. Both the high percentage of non-silicate material, including a likelihood of a nontrivial carbonaceaous component (Neri et al., 2019), result in a relatively low RI density. *** conclude on relevance to sf topo***

Enceladus is a much smaller moon with an estimated RI radius of 180 km (McKinnon, 2013). Thermal and orbital evolution models suggest that heat generated by accretion, radioactive decay, and/or tidal dissipation would be transferred before the temperature was high enough to melt a silicate interior (e.g. Neveu and Rhoden, 2019; Sotin et al., 2009). Thus, Enceladus is interpreted to have a porous, granular RI with ice/water filled pores (Roberts, 2015) and we do not expect volcanic features on the seafloor of this small OW.

If faulting of the outermost RI occurs on an OW, sustained slip along fault planes could generate bathymetric relief. Past convection of the RI may have produced faulting on moderate-large OWs. On Europa, deformation of the upper thermal boundary layer (Béhounkova et al., 2021) early in the body's history could have resulted in brittle failure and fault displacement. If RI convection was accompanied by upper boundary layer motion (plate drift) then residual seafloor relief could exist where rifting or collision occurred. Periodic tidal strains on Titan, Europa and Enceladus could also result in present-day RI fracturing or dislocations. If heterogeneities in the RI cause local stress concentrations or asperities, these periodic strains could produce a ratcheting effect where slip is easier in one direction and fault offset could accrue. The pattern of large-scale rifting in the ice shells of some icy moons, show that tidal forcing can create sustained, large-scale fractures with a variety of orientations, that do not appear and disappear across tidal cycles. Seafloor forces, despite being smaller than what the ice shell experiences, would be subject to the same physics and the greater rigidity of the RI would amplify and sustain the influences of heterogeneity relative to ice. Compared to Earth, cyclic body tides on many OWs are very large. Given expected material properties for the RIs of Europa, Titan, and Enceladus (Table 1), displacement responses could be on the order of ~10 m (Enceladus) to a few m (Europa), assuming that much of the planetary tidal dissipation occurs in the RI instead of the ice shell (McCarthy and Castillo-Rogez, 2011; Randolph-Flagg et al., 2020). The influence of modest scale seafloor relief on hydrothermal circulation would likely be most important in terms of the development of preferential fluid and heat flow paths within the fault displacement zones.

Meteorite impacts are another potential source of bathymetric relief on OWs. On Earth, the Chicxulub asteroid impact off the Yucatan peninsula occurred through a 3.5 km-deep ocean and created seafloor crater rim heights of 100's-1000 m and an outer rim diameter of ~100 km (Morgan et al., 1997). Impacts of this size have been relatively rare in recent Earth history and, given that most of the lithospheric surface below the ocean is < 150 M.y. in age, there are few comparable records. However, when such impacts do occur, we now know that the residual topographic anomalies host sustained subseafloor hydrothermal circulation [Kring et al., 2020]. The active ice shells of Titan, Europa, and Enceladus similarly preclude development of a long-term impact history on these OW, but we expect that these bodies would have been hit multiple times by impactors large enough to disrupt the seafloor since they formed (Zahnle et al., 2003). However, once the hydrosphere of these OWs exceeded a few km in thickness, seafloor impact by meteorites would have been greatly reduced. Strikes by moderate-large meteors that occurred before the hydrosphere thickness was greater than a few km could have resulted in formation of impact craters with narrow rims and heights on the order of km.

Subsequent differentiation of the silicate:ice interior was likely slow enough that disruption of the seafloor would have been modest, although sediments/debris could collect on the seafloor around and within a crater, reducing local relief over time.

Earth, Titan and Europa, and Enceladus have gravitational acceleration at their seafloors ranging from 1*g* to ~0.1 *g* to ~0.01*g*, respectively. These differences have consequences for the evolution of seafloor features, as the load imposed on the seafloor by bathymetric highs scales with gravity. The deformation rate of the seafloor in response to the load could scale with gravity as well, depending on the mechanism(s). Low gravity on Enceladus helps to limit pressure at the seafloor (< 50 MPa) and aid in retention of porosity inherited from accretion and differentiation processes over geological timescales (Neveu and Rhoden, 2015). Thus, the granular RI is expected to be relatively weak (e.g., Choblet et al., 2017; Palguta et al., 2010; Roberts, 2015). Higher gravity OWs like Europa and Titan are expected to have more complex RI rheology resulting from silicate differentiation and/or alteration and to experience seafloor deformation rates that are similar to that of Earth's seafloor.

3. Support of bathymetric loads: Analytic Model Estimates

On Earth, a model of temperature-dependent plate rigidity and 2-D plate flexure can explain several fundamental seafloor observations: steady deepening and thickening of the oceanic lithosphere with distance from a spreading center and the associated reduction in heat flow (Parsons & Sclater, 1977; Stein and Stein, 1992); the wavelength and amplitude of outer-rises that typically precede plate subduction into a trench (Caldwell et al., 1979); and moats that surround large seamounts/islands as well as their residual topography (Bodine et al., 1981; Detrick and Crough, 1978). We first explore whether an OW having an outermost rocky interior that is more rigid than the underlying material could support km-scale relief.

Temperature exerts a strong control on silicate rock strength, with Earth's oceanic lithosphere behaving elastically at temperatures below 600-800°C (e.g. Bergman and Solomon, 1984; McNutt, 1984). At temperatures greater than 1000°C, ductile deformation of silicate rock is dominant (Nicolas and Poirier, 1976). Subseafloor thermal gradients on Europa have been estimated to range from 3-180°C/km (Béhounkova et al, 2021; Lowell and DuBose, 2005) which would translate to a RI having a rigid outer layer with thickness of ~5.6-270 km. The average temperature gradient in one model of Enceladus (Choblet et al., 2017) is ~1.5°C/km, which would correspond to a fully elastic interior if crystalline silicate dictates the physical properties. However, high porosity and ice fraction in the rocky interior of this OW (possibly ≥20%; Roberts, 2015), would tend to weaken material properties by up to several orders of magnitude, especially if there is long-term loading (e.g. Nimmo, 2004). Instead, diagenesis may dominate the degree of rigidity within the immediately sub-seafloor layer of Enceladus. Water-rock reactions result in mineral alteration and cement formation, binding grains, and potentially occluding porosity so the affected layer becomes stiffer than underlying (ice-filled) granular material. Alteration processes may also limit the depth extent of the most vigorous seawater circulation if pore spaces fill completely during remineralization. Titan probably falls in between the Europa and Enceladus scenarios for rigid vs ductile behavior as discussed in Section 4.

While the thermal and diagenetic state of an OW could reasonably result in a layered RI that is more rigid near the seafloor and more ductile at depth, there is considerable uncertainty in material properties of the seafloor layer. The extent to which melt that formed in Europa's silicate interior in the past was able to segregate and rise to the surface is unknown, so the density of the outermost RI is uncertain. The range of the elastic moduli, on the other hand, is likely close to Earth if the seafloor is crystalline rock. Knowledge of Titan is still developing so for our analytic models we adopt published values for the expected ice/silicate RI. Uncertainty is even greater for Enceladus due to its inferred porous, granular character. If diagenesis has been robust, the seafloor layer could deform elastically, reflecting the strength of the binding secondary mineralization (e.g., Hemmerle et al., 2016) but the depth extent of such reactions could be limited, resulting in a rather thin rigid layer (e.g. < 1 km). If Enceladus' seafloor retains a granular nature, the response to modest, steady loads could still be elastic, as has been shown to be the case for Earth sands and sandy soils under certain conditions (e.g. Lade and Nelson, 1987; Wood, 1998). However, a response resulting in permanent strain is also relevant (e.g. Lade and Kim, 1988; Wood, 1998). To address the uncertainty in mechanical behavior, we test a suite of parameter values that encompass a range that prior publications indicate could be relevant for Titan, Europa, and Enceladus (Table 1). We consider first an elastic plate model and then a viscous layer model.

The basic concept of thin elastic plate flexure theory applied beneath an ocean (Turcotte and Schubert, 1982) is that a rigid seafloor layer overlies ductile material of the deeper interior. If local topography loads the plate, its inherent strength may support the load indefinitely, or the plate may bend (deflect) under the load (Figure 2). If the plate is not strong enough, it deforms (relaxes), local isostatic compensation prevails and most of the original relief is eventually eliminated (Airy isostasy). The density contrast between the rigid and ductile material determines how much relief remains. The size of the load is a key factor in the plate's deflection or compensation response.

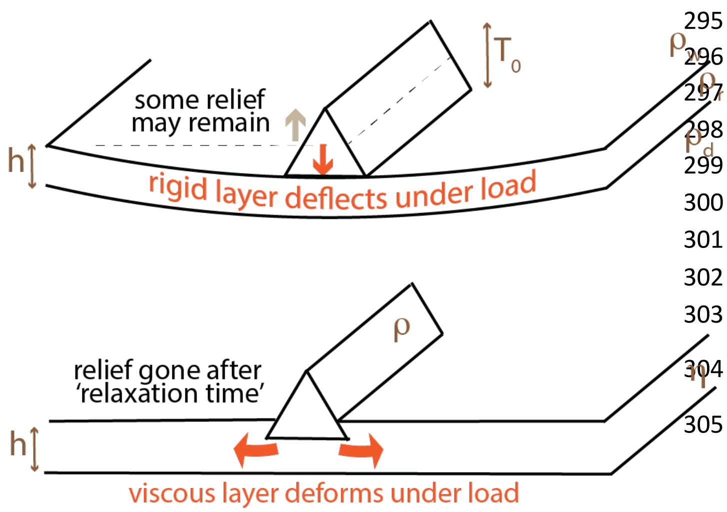

Figure 2. Two-dimensional model of a bathymetric load, black triangle of height T_0. (upper) elastic plate of thickness h and density ρ_r (same as load) , overlain by seawater of density ρ_w and underlain by ductile material of density ρ_d. (lower) Load of density ρ on layer with viscosity η and thickness h.

For a 2-D case (Figure 2) with no lateral tectonic forces acting on a plate, deflection beneath the center of a bathymetric load is (Turcotte and Schubert, 1982):

$w_o = \frac{V\alpha^3}{8D}$ for a line load (extending out of plane), where $V = (T_0)^2 \rho_r g/2$ is the weight of the load.

$w_0 = \frac{T_0}{\left[\frac{D}{g\rho_r}\left(\frac{2\pi}{\lambda}\right)^4 + \frac{\rho_d}{\rho_r} - 1\right]}$, for a periodic load of wavelength λ.

where the flexural parameter is $\alpha = \left\{\frac{4D}{g(\rho_d - \rho_w)}\right\}^{\frac{1}{4}}$, the flexural rigidity is $D = \frac{Eh^3}{12(1-\nu^2)}$, E is Young's modulus, ν is Poisson's ratio, and g is gravitational acceleration.

The application of this simple (rectangular) plate model provides an end member case with an analytic solution. Our intent here is to obtain limits on possible response, rather than to simulate a specific feature geometry, load distribution, or RI properties.

We assess how plate strength, as characterized by Youngs modulus and Poisson's ratio, and layer densities affect the predicted topographic support or compensation, focusing on load heights of 100 m to 3 km. We calculate results for a wide range of possible plate thickness: 1-100 km on Europa and Titan; 10 m-10 km on Enceladus. We compare the plate deflection that a given topographic load would produce for scenarios relevant to Earth, Titan, Europa, and Enceladus. Ocean density is assumed to be 1030 kg/m^3 except for on Titan where values 1150-1190 kg/m^3 were tested.

Table 1. Material properties for the rocky interior of selected ocean worlds.

Earth	**Europa**	**Titan**	**Enceladus**
Rocky Interior radius (r)= 6374 km	RI r =1374-1411 km	RI r = 1850-2116 km	RI r = 190-195 km
E=5.7 x 10^{10} Pa	G=5 x 10^{10} Pa, E=2(1+ν)G	G=9 x 10^9 Pa	$G_{effective}$ = 10^7 - 10^8 Pa
ν = 0.25-0.30	ν = 0.25-0.30	ν = 0.29-0.33	ν = 0.15-0.27
g = 9.81 m/s^2	g = 1.31 m/s^2	g = 1.35m/s^2	g = 0.114 m/s^2
ρ_r = 2750-3150 kg/m^3	ρ_r = 2990-3300 kg/m^3	ρ_r = 2565-2975 kg/m^3	ρ_r = 2450-2600 kg/m^3
ρ_d = 3300-3400 kg/m^3	ρ_d = 3300 kg/m^3	ρ_d = 2565-2975 kg/m^3	ρ_d = 2450-2600 kg/m^3
η = 10^{18}-10^{22} Pa s	η = 10^{16} (seds)-10^{19} (fractured) Pa s	η = 10^{23} Pa s	η = 10^{14}-10^{16} Pa s (granular RI)
Turcotte & Schubert, 1982	*Hussman et al., 2016; Behounkova et al., 2021; Cloos & Shreve, 1988*	*Nimmo ***; Sotin et al., 2021; Howell & Pappalardo, 2018*	*Choblet et al., 2017; Lade & Nelson, 1987*

Line loads that are 0.5-1 km high and wide are not predicted to deflect the plate by an amount that would significantly reduce bathymetric relief, except for the thinnest plates (<1 km) on Enceladus, where deflection of more than 100 m is predicted for the cases tested. Loads 3 km and larger could cause deflection of several hundred m for a very thin plate (1 km) on

Europa. On Titan, Enceladus (and Earth) a 3 km load could cause 500-800 m deflection, or more, a significant fraction of the feature's height, but only if the plate is very thin (≤1 km). The uncertainty in Titan's Poissons ratio has negligible effect on the predicted deflection; minimizing the difference in rigid versus ductile layer density shifts Titan's predicted deflection higher, essentially equal to that for Earth. For Europa and Enceladus (Figure 3), uncertainty in Poisson's ratio has only slight influence on deflection. Uncertainty in density of the ductile layer has modest effect. Shear modulus has a more important effect on predicted deflection .

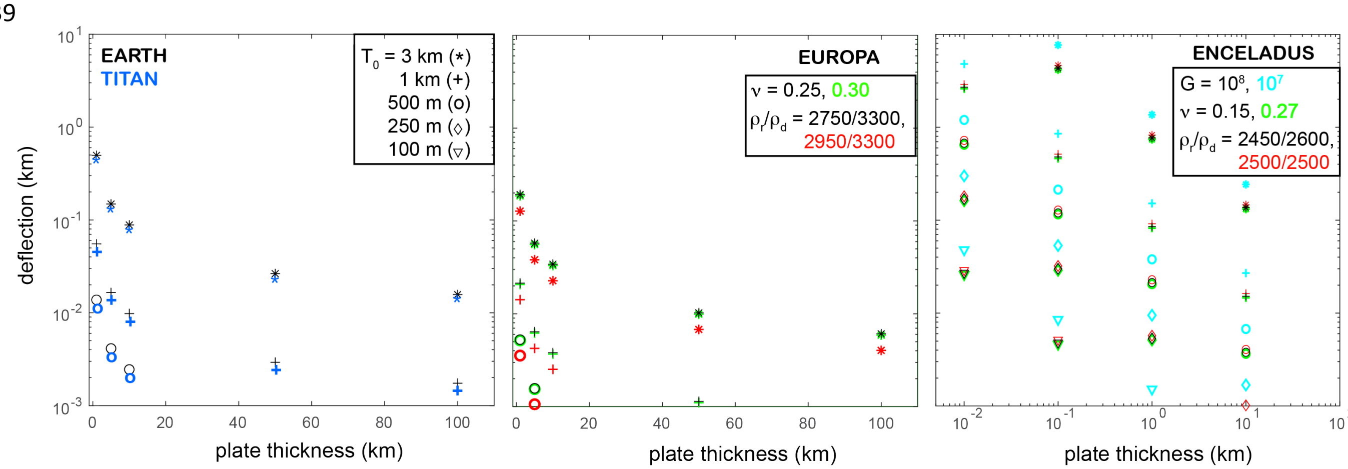

Figure 3. Maximum deflection for various plate thicknesses due to various sizes (T_0) of linear bathymetric loads (different symbols). Note the log scale for Enceladus where plates <1 km thick were also considered. Symbol color (right 2 panels) indicates plate properties for each calculation, as listed in each legend.

Thin plate theory shows that there is a wavelength dependence of support versus compensation for periodically distributed topographic loads. We focus here on the width of bathymetric features for which plate behavior over geologic time scales is described. Topographic feature wavelengths that are below (to the left, Figure 4) of the sharp rise in the curves are fully supported by the plate's strength and could persist over long times. As feature width increases, there is a range for which the loads are partially compensated, evident where the curves rise steeply and deflection approaches load height. Where the curves flatten beyond this transition, at longer wavelengths, loads are fully compensated.

Periodically spaced seafloor relief at km-scale wavelength and amplitude could be supported by a rigid layer that is 1 km thick or greater (Figure 4). Plate deflection for features with wavelengths of 10's-100's km would exceed the criteria for long-term persistence in this model except where plate thickness is on the order of 100 km. For Enceladus, where a re-mineralized rigid seafloor layer may be rather thin (≤ 1 km), only small amplitude periodic relief could be supported at wavelengths that are commensurate with the respective plate thickness (Figure 4).

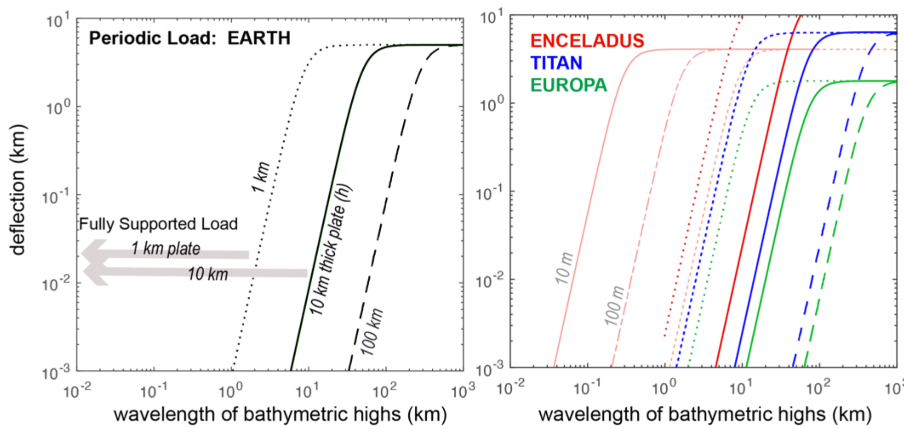

Figure 4. Deflection due to a periodic load on a rigid plate with thickness h, labeled by line type. left) Earth. right) Other OW as indicated by color. Most cases shown assume topographic amplitude is 1 km. For Enceladus, opaque red curves are for 250 m load amplitude.

Alternatively, if the outermost RI of an OW is extensively fractured due to tidal strains or if thick sediment has accumulated, a model where the seafloor layer behaves with an effective viscosity may be more appropriate. In this scenario, the persistence of bathymetric relief results from the internal resistance to deformation under the weight/distribution of the load (*e.g.,* Thomas and Schubert, 1986). The 'relaxation' rate of the load is determined by an effective viscosity based on the aggregate behavior of the layer as a function of load wavelength (λ).

The relaxation of topography is given by an e-folding time (τ) with general form (*Cathles, 1975)*:

$$\tau = \frac{2\eta}{\rho g h}\frac{cosh^2\left(\frac{h}{\lambda}\right)+\left(\frac{h}{\lambda}\right)^2}{cosh\left(\frac{h}{\lambda}\right)sinh\left(\frac{h}{\lambda}\right)-\frac{h}{\lambda}}$$

where η is the effective viscosity of the layer with thickness, *h*, and density, ρ. For topography much narrower than the viscous layer thickness (Haskell, 1935):

$$\tau_{\lambda \ll h} = \frac{2\eta}{\rho g \lambda}$$

For very wide topographic loads, relative to viscous layer thickness (Jeffreys, 1952):

$$\tau_{\lambda \gg h} = \frac{3\eta\lambda^2}{\rho g h^3}$$

This viscous representation provides a useful gauge to compare the scale of the difference in km-scale load support to that predicted by the elastic plate model. A plastic model could predict even greater difference, depending on the mechanisms included.

The viscous layer calculations for Europa and Enceladus indicate that, for a reasonable range of inferred properties (Table 1), topography with km-scale wavelengths would persist on M.y. timescales only if the extensively fractured, or thickly sediment covered, seafloor layer is thin (100's m, Figure 5). Because of the lower gravity, bathymetric relief on Enceladus would persist longer than on Europa for the same effective viscosity.

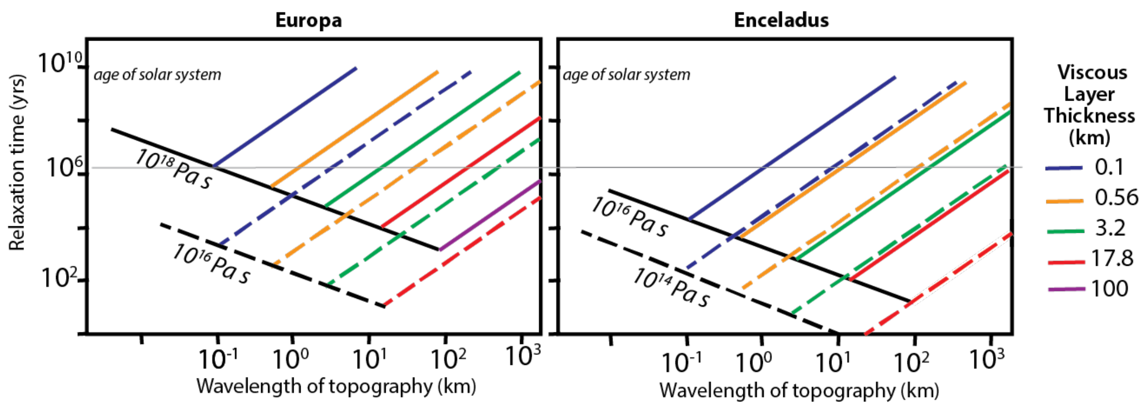

Figure 5. Viscous relaxation time for topographic features based on published RI viscosities. Dashed & solid lines indicate different effective viscosities of the seafloor layer. Color indicates layer thickness. Both approximations break down near the intersection of each colored line (Jeffreys approximation) and the black line (Haskell), as λ approaches the magnitude of *h*.

Viscous relaxation models are commonly used to explain residual topography on ice shells (*e.g.*, Parmentier and Head, 1981), dynamic topography of the continental crust in the aftermath of glaciation and earthquakes (*e.g.*, Cathles, 1975), and in geomorphic models of granular or fractured materials (*e.g.*, Ferdowski et al., 2018). In contrast, compensation of seafloor topography on Earth has been shown to reflect variations in local crustal thickness and is better explained by support due to an underlying stiff mantle layer (Neumann and Forsyth, 1993).

These analytic models are highly idealized, both in terms of their Cartesian geometry and assumed deformation style. The intent has been to illustrate that at least some scenarios predict peristence of km-scale seafloor relief over geologic time scales: most likely for Europa; generally unlikely Enceladus but 100'sm sized features could presist; Titan falls between these two cases for the rigid plate with periodic relief and, in the next Section, we consider load-induced deformation on a spherical seafloor and viscous RI for this OW.

4. Titan response to seafloor load: Numerical model estimate *(Sotin & Barbey)*

5. Discussion

5.1 Possible Scales of Bathymetric Relief on Ocean Worlds

The simple analytic model results show that the seafloor of an OW with elastic properties that could be relevant for Titan, Europa, or Enceladus would support narrow (< 3 km), linear bathymetric features of 0.5-1 km height, if the RI has an outermost rigid layer overlying more ductile material. Linear loads 3 km and larger would be partially to fully compensated on Enceladus if the rigid seafloor plate were very thin (≤ 1 km). On Earth, effective elastic plate thickness this low has been calculated for regions of major, recent extension (e.g. Buck, 1988; Reston and Ranero, 2011). For periodically distributed bathymetric relief of 1 km amplitude, seafloor features narrower than 5 km would be supported for all OW material properties tested (Table 1) unless the rigid layer were less than 5 km thick. On Europa, even a very thin (1 km) plate would support a periodic load up to 3 km wide. In contrast, complete compensation of 1 km high relief could occur on Enceladus if the rigid seafloor layer were ~1 km thick. Loads wider than 20 km are predicted to be fully compensated on both these OW, resulting in much less residual bathymetric relief.

If the OW seafloor layer lacks rigidity due to ongoing, extensive fracturing, significant alteration, or thick sediment, km-scale bathymetric relief would not persist for Enceladus conditions, but it could persist on Titan and Europa. Wider features (> 10 km wavelength) could persist on Europa if the layer were ~3 km thick, or on Enceladus if they were >100 km wide for similar layer thickness.

In summary, km-scale bathymetric relief on OWs such as Titan, Europa and Enceladus is not precluded. Consideration of potential sources of bathymetric relief (Section 2) suggests that km-scale features could have been generated at various times during OW evolution. Our analytic and numerical calculations (Sections 3 and 4) suggest that such features could be supported over geologic time scales, even if the deep interior of an OW were not rigid over the same period, if there were an outermost layer of the rocky interior that is relatively stiff, with mechanical properties that fall within a reasonable range.

5.2 Implications for Hydrothermal Circulation on Ocean Worlds

On Earth, bathymetric relief of km scale is associated with conductive refraction of subseafloor isotherms, often increased local basement permeability, and variations in the thickness of seafloor sediment (and thus connectivity between the ocean and the crustal hydrothermal aquifer). Each of these factors can impact the development of thermally-significant rates of fluid recharge, discharge, and lateral flow within hydrothermal systems across a range of temperatures and spatial scales.

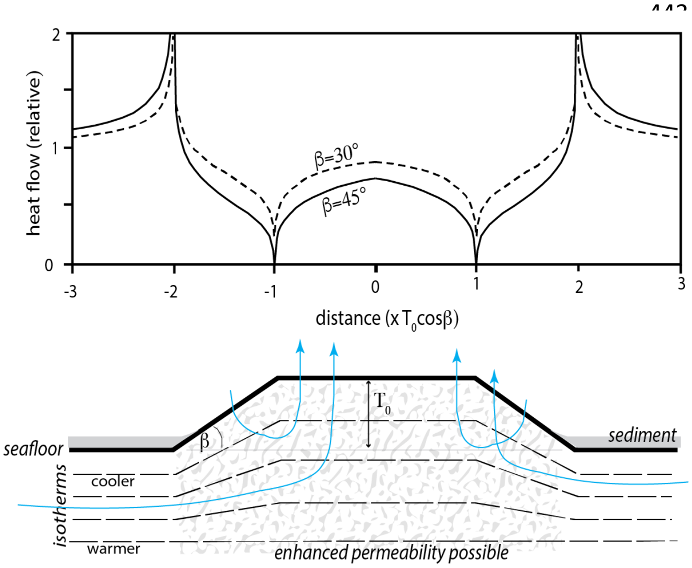

Figure 6. Conductive refraction due to warping of isotherms by bathymetric relief results in variations in heat flow through the seafloor (after Lachenbruch, 1968). Gray shades in the lower panel illustrate possible lateral variations in ocean:interior connectivity due to sediments (solid gray), and/or permeability (mottled) associated with a bathymetric feature. Blue arrows suggest possible hydrothermal flow paths (e.g., Hutnak et al., 2006; Kawada et al., 2011). Additional heat flow deviations associated with convection are not plotted above

Even without fluid flow, seafloor relief plays an important role in focusing conductive heat. The seafloor in the deep ocean is at essentially constant temperature distant from magmatically active areas so shallow isotherms tend to spread out beneath bathymetric highs (Lachenbruch, 1968; Figure 6). This local change in subseafloor thermal gradient is caused by conductive refraction, resulting in reduced heat flux above the feature and elevated heat flow along the edges. The extent of the refraction is positively correlated with the magnitude of the relief and the local seafloor slope. This effect is purely conductive, is always expected, and can be amplified if accompanied by lateral variation in seafloor hydrologic connectivity (sediment cover) or basement permeability that results in significant advective heat transport.

We expect that the outermost RI of an OW will have non-zero porosity, and mechanisms that generate bathymetric relief may also lead to local increase in subseafloor permeability (Section 2). Silicates exposed to seawater react to form alteration minerals. This can seal hydrothermal pathways, as has been documented in oceanic basalts on Earth (Alt, 2004; Bartetzko and Fisher, 2008). In olivine-rich plutonic rock, volume expansion accompanies serpentinization, causing local microfractures to develop and generating secondary porosity (Schwarzenbach, 2016). Thus, there can be competing alteration processes leading to increases or decreases in outcrop porosity and permeability, depending on rock and fluid temperature and chemical compositions, fluid flow rates and residence times. Ongoing tidal flexing of the outermost RI of OW may also help maintain subseafloor permeability.

Marine sediments generally have low permeability (e.g., Bryant et al., 1974; Langseth et al., 1992; Spinelli et al., 2004) and driving forces for fluid flow tend to be small, so hydrothermal seepage through sediments is usually modest. The extent of ocean sedimentation on OW is unknown but there are several possible sources: precipitation from the ocean itself (Daswani et al., 2020); erosion and segregation of granular RI material (e.g., Ottino and Khakhar, 2000); deposition of meteoritic material that is efficiently cycled through a convecting ice shell (Randolph-Flagg et al, 2023). Importantly, without the rapid recycling of OW seafloor by plate tectonics or other processes, even very slow rates of sediment accumulation could result in significant thickness over geologic time.

On Earth, marine sediments generally infill between topographic features or accumulate in local depressions, rather than uniformly draping the seafloor. Whether this will be the case on an OW will depend on particle size and the flow rates of ocean currents near the seafloor. OW ocean currents have been modeled (Kang et al., 2021; Lobo et al., 2021; Soderlund, 2019) with flow rates ranging from mm/s to m/s, similar to bottom currents on Earth's seafloor. As bottom currents interact with km-sized topographic features, constriction of the water mass and corresponding increase in local flow speed will occur, thereby increasing the capacity of currents to carry sediments. Differences in sedimentation rates over bathymetric highs and lows could result as a consequence (e.g. McCave and Hall, 2006).

6. Summary

We find that the existence of seafloor relief cannot be ruled out on the basis of current knowledge of rocky interior properties on Titan, Europa, and Enceladus. There are mechanisms that could reasonably create topographic variation during the evolution of each body, if not present day, and our calculations indicate that km-scale relief could persist long term on Europa and Titan. Persistence on Enceladus is unlikely although scenarios with a thin rigid seafloor layer resulting from diagenetic cementation could support modest relief. While the km-scale bathymetric relief considered in this study is 1-2 orders of magnitude smaller than what can be observed with current or planned OW data, ignoring the possibility of its existence could significantly bias predictions for the mode and magnitude of hydrothermal exchange.

Bathymetric relief that is not covered by low-permeability sediment can expose areas of the silicate interior of an OW. Seawater penetration and reaction are likely to occur as a consequence as long as there are permeable pathways, particularly if the system is heated internally or from below. Lateral variations in the thermal gradient due to conductive refraction and small pressure differences associated with seafloor morphology can influence flow rates and patterns of fluid circulation. Over time, the regional vertical thermal gradient and the magnitude of the difference in area/permeability of the exposed highs and the surrounding seafloor will determine whether robust hydrothermal circulation will develop.

Our aim in exploring the possibility of km-scale OW bathymetric relief is to develop framework that can guide complementary investigations into hydrothermal circulation in their RIs (German et al., 2022). Observation of Earth's sub-seafloor hydrothermal systems shows that seafloor heterogeneity has a strong influence on patterns of in/outflow. Modeling, seismically-constrained porosity:depth profiles, and consideration of the heat balance measured in plumes all suggest that a majority of Earth's seafloor hydrothermal flow occurs within the upper few kilometers of the solid interior. We conclude that it will be worthwhile to consider models of hydrothermal circulation on OWs where bathymetric relief at a scale of kilometers might influence the circulation of ocean fluids within the outermost rocky interior. Such results could provide important perspective, in concert with global-scale model outputs, to advance understanding of thermal and chemical exchange that could occur on other OW, and, hence, their biological potential.

Acknowledgements. This work was supported by NASA grant 80NSSC19K1427 and National Science Foundation grants OIA-0939564 and OCE-1924384. Valuable general insights on OWs have been provided throughout discussions with our full collaborative project group (ExOW, https://oceanworlds.whoi.edu/exploring-ocean-worlds-exow-team-members/), which we also acknowledge as informing the development of this work.

References.

Alt, J.A. (2004) Alteration of upper oceanic crust: mineralogy, chemistry and processes, in *Hydrogeology of the oceanic lithosphere* E.E. Davis and H. Elderfield (eds.) Cambridge Univ. Press, p 456-488.

Anderson, B.W., L.A. Coogan, K.M. Gillis (2012), The role of outcrop-to-outcrop fluid flow in off-axis oceanic hydrothermal systems under abyssal sedimentation conditions, *J. Geophys. Res.*, *117*(B5), B05103, doi:05110.01029/02011JB009052.

Bartetzko, A. and A.T. Fisher (2008) Physical properties of young (3.5 Ma) oceanic crust in the eastern flank of the Juan de Fuca ridge: Comparison of wireline and core measurements with global data, J. Geophys. Res. 113, doi:10.1029/2007JB005268.

Běhounková, M., G. Tobie, G. Choblet, M. Kervazo, M. Melwani Daswani, C. Dumoulin, S.D. Vance, (2021) Tidally induced magmatic pulses on the oceanic floor of Jupiter's moon Europa. Geophys. Res. Lett. 48, doi: 10.1029/2020GL090077 .

Baker, P.A., P.M. Stout, M. Kastner, H. Elderfield (1991) Large-scale lateral advection of seawater through oceanic crust in the central equatorial Pacific, Earth Planet. Sci. Lett. 105 doi:10.106/0012-821X(91)90189-O.

Bergman E.A. and S.C. Solomon (1984) Source mechanisms of earthquakes near mid-ocean ridges from body waveform inversion: Implications for the early evolution of oceanic lithosphere, J. Geophys. Res 89, doi:10.1029/JB089iB13p11415.

Bodine, J.H., M.S. Steckler, A.B. Watts (1981) Observations of flexure and the rheology of the oceanic lithosphere, J. Geophys. Res. 86, doi:10.1029/JB086iB05p03695.

Bryant, W. R., A.P. Deflanche, P.H. Trabant (1974) Consolidation of marine clays and carbonates, in Deep-sea sediments, physical and mechanical properties, edited by Inderbitzen, A. L., pp. 209-244, Plenum Press, New York.

Buck, W.R. (1988) Flexural rotation of normal faults, Tectonics 7, doi:10.1029/TC007i005p00959.

Cadek, O., K. Kalousova, J. Kvorka, C. Sotin (2021) The density structure of Titan's outer ice shell; Icarus 364, doi: 10.1016/j.icarus.2021.114466

Caldwell, J.G., W.F. Haxby, D.E. Karig, D.L. Turcotte (1976) On the applicability of a universal elastic trench profile, Earth. Planet. Sci. Lett. 31, 239-246.

Cann, J. and M.R. Strens (1989) Modeling periodic megaplume emission by blavk smoker systems, J. Geophys. Res. 94, doi: 10.1029/JB094iB09p12227.

Carbotte, S.M., J-P. Canales, M.R. Nedimovic, H. Carton, J.C. Mutter (2012) Recent seismic studies at the East Pacific Rise 8z820'-10Z810'N and Endeavour segment: Insights into mid-ocean ridge hydrothermal and magmatic processes, Oceanography 25, 100-112, doi: 10.5670/oceano.2012.08.

Cathles, L.M. (1975) Viscosity of the Earth's Mantle, Princeton Univ. Press.

Choblet G., G. Tobie, C. Sotin, M. Behounkova, O. Cadek, F. Postberg, O. Soucek (2017) Powering prolonged hydrothermal activity inside Enceladus, Nat. Astro. 1, 063, doi:10.1038/s41550-017-0289-8.

Clague, D.A., J.F. Martin, J.B. Paduan, D.A. Butterfield, J.W. Jamieson, M Le Saut, D.W. Caress, H. Thomas, J.F. Holden, D.S. Kelley (2020) Hydrothermal chimney distribution on the Endeavour segment, Juan de Fuca ridge, Geochem. Geophys. Geosys. 21, doi: 10.1029/2020GC008917.

Cloos, M., and Shreve, R., 1988, Subduction channel model of prism accretion, melange formation, sediment subduction, and subduction erosion at convergent plate margins: 1. Background and description: Pure and Applied Geophysics 128, p. 455-500.

Daswani, M.M. and S.D. Vance (2020) Evolution of volatiles from Europa's interior into its ocean, Goldschmidt Conference Abs. doi: 10.46427/gold2020.1777 .

Davies, J.H. and D.R. Davies (2010) Earth's surface heat flux, Solid Earth 1, 5-24.

Davis, E., Fisher, A. T., Firth, J. V., Andersson, E. M., Aoike, K., Becker, K., ... & Miller, A. T. (1992). Initial Reports. In *Proceedings of the Ocean Drilling Program* (Vol. 139).

Davis, E. E., et al. (1992), FlankFlux: an experiment to study the nature of hydrothermal circulation in young oceanic crust, *Can. J. Earth Sci.*, *29*(5), 925-952.

Delaney, J.R., Kelley, D., Lilley, M., Butterfield, D., Mcduff, R., Baross, J., Deming, J., Johnson, H., Robigou, V. (1997) The Endeavour hydrothermal system I: Cellular circulation above an active cracking front yields large sulfide structures, 'fresh' vent water, and hyperthermophilic archaea, RIDGE Events. 8. 11-19.

deMartin, B.J., R.A. Sohn, J-P. Canales, S.E. Humphris (2007) Kinematics and geometry of active detachment faulting beneath the TAG hydrothermal field on the Mid-Atlantic Ridge, Geology 35, doi:10.11230/G23718A.1.

Detrick, R.S. and S.T. Crough (1978) Island subsidence, hot spots, and lithospheric thinning, J. Geophys. Res 83, 1236-1244.

Dunn, R.A. and D.W. Forsyth (2003) Imaging the transition between the region of mantle melt generation and the crustal magma chamber beneath the southern East Pacific Rise with short-period Love waves, J. Geophys. Res. 108, doi: 10.1029/2002JB002217.

Elderfield, H. and A. Schultz (1996) Mid-ocean ridge hydrothermal fluxes and the chemical composition of the ocean, Ann. Rev. Earth Planet. Sci. 24, doi: 10.1146/annurev.earth.24.1.191.

Ferdowski, B., C.P. Ortiz, D.J. Jerolmack (2018) Glassy dynamics of landscape evolution, PNAS 115, doi: 10.1073/pnas.1715250115.

Fisher, A.T., E.E. Davis, M. Hutnak, V. Spiess, L. Zuhlsdorff, A. Cherkaoui, L. Christiansen, K.M. Edwards, R. Macdonald, H. Villinger, M. Mottl, C.G. Wheat, K. Becker (2003) Hydrothermal circulation across 50 km on a young ridge flank: the role of seamounts in guiding recharge and discharge at a crustal scale, Nature 421, 618-621.

Fisher, A. T., and R. Harris (2010), Using seafloor heat flow as a tracer to map subseafloor fluid flow in the ocean crust, Geofluids, doi: 10.1111/j.1468-8123.2009.00274.x

German, C.R. and W.E. Seyfried (2014) Hydrothermal Processes, Chapter 8.7 in HD Holland and KK Turekian, Treatise on Geochemistry, 2nd edition, Elsevier, doi: 10.1016/B978-0-08-095975-7.00607-0.

C.R.German, S.Q.Lang, J.N.Fitzsimmons (2023) Hydrothermal Processes *In*: Treatise of Geochemistry, 3rd Edition. Elsevier, in review.

Goff, J.A., W.H.F. Smith, K.M. Marks (2004) The contributions of abyssal hill morphology and noise to the altimetric gravity fabric, Oceanography 17, 24-37.

Green, A.P., C.M. Elder, M.T. Bland, P. Tackley (2023) Strong lithospheric resistance limits potential for Europan seafloor volcanism, AGU Fall Mtg abstract P41G-3256.

Hand, K.P., Sotin, C., Hayes, A. *et al.* On the Habitability and Future Exploration of Ocean Worlds. Space Sci Rev. 216, 95 (2020). https://doi.org/10.1007/s11214-020-00713-7.

Hand, K.P. and C.R. German, (2018) Exploring ocean worlds on Earth and beyond. Nature Geoscience. Vol. 11:1, doi: 10.1038/s41561-017-0045-9.

Haskell, N. A., The motion of a fluid under a surface load, Physics, 6, 265-269, 1935.

Hasterok, D. (2013), Global patterns and vigor of ventilated hydrothermal circulation through young seafloor, Earth Planet. Sci. Lett. 380, 12-20, doi: 10.1016/j.epsl.2013.08.016.

Haymon, R.M., D.J. Fornari, M.H. Edwards, S. Carbotte, D. Wright, K.C. Macdonald (1991) Hydrothermal vent distribution along the East Pacific Rise crest (9°09'-54'N) and its relationship to magmatic and tectonic processes on fast-spreading mid-ocean ridges, EPSL 104, doi:10.1016/0012-821X(91)90226-8.

Hemingway, D.J. and T. Mittal (2019) Enceladus's ice shell structure as a window on internal heat production, Icarus 332, doi: 10.1016/j.icarus.2019.03.011.

Hemmerle, A., M. Schröter, L. Goehring (2016) A cohesive granular material with tunable elasticity, Sci. Rpt. 6, 35650, doi: 10.1038/srep35650.

Hendrix, A.R., T.A. Hurford, L.M. Barge, M.T. Bland, J.S. Bowman, W. Brinckerhoff, B.J. Buratti, M.L. Cable, J. Castillo-Rogez, G.C. Collins, S. Diniega, C.R. German, A.G. Hayes, T. Hoehler, S. Hosseini, C.J.A. Howett, A.S. McEwen, C.D. Neish, M. Neveu, T.A. Nordheim, G.W. Patterson, D.A. Patthoff, C. Phillips, A. Rhoden, B.E. Schmidt, K.N. Singer, J.M. Soderblom, S.D. Vance (2019) The NASA Roadmap to Ocean Worlds.Astrobiology, 1-27 doi: 10.1089/ast.2018.1955.

Hsu, H.W.., Postberg, F., Sekine, Y. (2015) Ongoing hydrothermal activities within Enceladus. Nature 519**,** 207–210 doi: 10.1038/nature14262.

Humphris, S.E., R.A. Zierenberg, L.S. Mullineaux, R.E. Thomson (1995) Seafloor hydrothermal systems, Geophys. Mono. 91, AGU.

Hussmann, H., C. Sotin, J.L. Lunine (2015) Interiors and evolution of icy satellites, Chap 10.18 in Treatise on Geophysics, 2nd edition doi:10.1016/B978-0-444-53802-4.00178-0.

Hussman, H., D. Shoji, G. Steinbrügge, A. Stark, F. Sohl (2016) Constraints on dissipation in the deep interiors of Ganymede and Europa from tidal phase-lags, CMDA 126, doi: 10.1007/s10569-016-9721-0.

Hutnak, M., A.T. Fisher, L. Zühlsdorff, V. Spiess, P.H. Stauffer, C.W. Gable (2006) Hydrothermal recharge and discharge guided by basement outcrops on 0.7–3.6 Ma seafloor east of the Juan de Fuca ridge: observations and numerical models. Geochem. Geophys. Geosyst. 7, doi: 10.1029/2006GC001242.

Hutnak, M., A.T. Fisher, R. Harris, C. Stein, K. Wang, G. Spinelli, M. Schindler, H. Villinger, E. Silver (2008) Large heat and fluid fluxes driven throuh mid-plate outcrops on ocean crust, Nature Geosci. 1, doi: 10.1038/ngeo264.

Jeffreys, H. (1952) The Earth: its origin and physical constitution, Cambridge Univ. Press. 393 p.

Johnson, H.P. and M.J. Pruis (2003) Fluxes of fluid and heat from the oceanic crustal reservoir, Earth Planet. Sci. Lett. 216, 565-574.

Kang, W., T. Mittal, S. Bire, J-M. Campin, J. Marshall (2021) Differing Enceladean ocean circulation and ice shell geometries driven by tidal heating in the ice versus the core, arXiv:2104.07008**.**

Kim, S.-S., and P. Wessel (2011), New global seamount census from altimetry-derived gravity data, *Geophys. J. Int.*, *186*(2), 615-631, 10.1111/j.1365-246X.2011.05076.x.

Kivelson, M.G., F. Bagenal, W.S. Kurth, F.M. Neubauer, C. Paranicas, J. Saur (2004) in *Jupiter, The Planet, Satellites, Magnetosphere*, ed. by F. Bagenal, T. Dowling, W. McKinnon (Cambridge Univ. Press, Cambridge), pp. 513–536.

Kawada, Y., N. Seama, and T. Urabe (2011), The role of seamounts in the transport of heat and fluids: Relations among seamount size, circulation patterns, and crustal heat flow, *Earth Planet. Sci. Lett.*, *306*(1-2), 55-65,

10.1016/j.epsl.2011.03.029
Koh, Z-W., F. Nimmo, J.L. Lunine, E. Mazarico, A.J. Dombard (2022) Assessing the detectability of Europa's seafloor topography from Europa Clipper's gravity data, Planet. Sci. J. 3:197, doi:10.3847/PSJ/ac82aa.
Kring, D.A., M.J. Whitehouse, M Schmieder (2021) Microbial Sulfur isotope fractionation in the Chicxulub hydrothermal system, Astobiology 21, doi: 10.1089/ast.2020.2286.
Lachenbruch, A.H. (1968) Rapid estimation of the topographic disturbance to superficial thermal gradients, Rev. Geophysics 6, 365-400.
Lade, P.V. and R.B. Nelson (1987) Modelling the elastic behaviour of granular materials, Num. Anal. Meth. Geomech. 11, doi: 10.1002/nag.1610110507.
Lade, P.V. and M.K. Kim (1988) Single hardening constitutive model for frictional materials III. Comparison with experimental data, Comp. Geotech. 6, 31-47.
Langseth, M.G., K. Becker, R.P. Von Herzen, and P. Schultheiss (1992), Heat and fluid flux through sediment on the western flank of the Mid-Atlantic Ridge: a hydrogeological study of North Pond, Geophys. Res. Lett. 19, 517-520
Lauer, R.M., A.T. Fisher, D.M. Winslow (2018) Three-dimensional models of hydrothermal circulation through a semount network on fast-spreading cruse, Earth Planet. Sci. Lett. 501, doi: 10.1016/epsl.2018.08.025.
Le Gal, V., F. Lucazeau, M Cannat, J. Poort, C Monnin, A. Battani, F. Fontaine, B. Goutorbe, F. Rolandone, C. Poitou, M-M. Blac-Valleron, A. Piedade, A. Hipolito (2018) Heat flow, morphology, pore fluids and hydrothermal circulation in a typical Mid-Atlantic Ridge flank near Oceanographer fracture zone, Earth Planet. Sci. Lett. 482, doi: 10.1016/j.epsl.2017.11.035
Lobo, A.H., Thompson, A.F., Vance, S.D., S. Tharimena (2021) A pole-to-equator ocean overturning circulation on Enceladus. *Nat. Geosci.* **14,** 185–189 doi: 10.1038/s41561-021-00706-3.
Lowell, R.P. and M. DuBose (2005) Hydrothermal systems on Europa, GRL 30, doi: 10.1029/2005GL022375.
McCave I.M. and I.R. Hall (2006) Size sorting in marine muds: processes, pitfalls, and prospects for paleoflow-speed proxies, G3 7, doi:10.1029/2006GC001284.
McCarthy, K. and J. Castillo-Rogez (2013) Planetary ices attenuation properties, in MS Guipati and J Castillo-Rogez (eds) The Science of Solar System Ices, p 183, Springer.
McKinnon, W.B. (2013) The shape of Enceladus as explained by an irregular core: Implications for gravity, librations, and survival of its subsurface ocean, J. Geophys. Res. 118, doi:10.1002/jgre.20122.
McNutt, M.K. (1984) Lithospheric flexure and thermal anomalies, J. Geophys. Res. 89, doi:10.1029/JB089iB13p11180.
Miller, N.C., D. Lizarralde, J.A. Collins, W.S. Holbrook, H.J.A. van Avendonk (2020) Limited mantle hydration by bending faults at the Middle America trench, J. Geophys. Res. 126, doi: 10.1029/2020JB020982.
Morgan, J., M. Warner and Chicxulub Working Group (1997) Size and morphology of the Chicxulub impact crater Nature 390, 472-476, doi: 10.1038/37291
Mottl M. J. (1989) Hydrothermal convection. reaction. and diffusion in sediments on the Costa Rica Rift flank: Porewater evidence from ODP Sites 677 and 678. *Proc. Ocean Drill. Prog., Sci. Results 111,* 195-213.
Mottl, M.J. (2003) Partitioning of energy and mass fluxes between mid-ocean ridge axes and flanks at high and low temperature, in *Energy and mass transfer in submarine hydrothermal systems*, edited by P. Halbach, V. Tunnicliffe and J. Hein, pp. 271-286, Dahlem University Press, Berlin, Germany.
Neri, A., F. Guyot, B. Reynard, C. Sotin (2019) A carbonaceous chondrite and cometary origin for icy moons of Jupiter and Saturn, Earth Planet. Sci. Lett. 530, doi: 10.1016/j.epsl.2019.115920.
Neumann, G.A. and D.W. Forsyth (1993) The paradox of the axial profile: Isostatic compensation along the axis of the Mid-Atlantic Ridge? J. Geophys. Res. 98, doi: 10.1029/93JB01550.
Neveu, M. & Rhoden, A. R. (2015) The origin and evolution of a differentiated Mimas. J. Geophys. Res. 296, 183–196.
Neveu, M. and A. Rhoden (2019) Evolution of Saturns mid-sized moons, Nature Astron. 3, 548-552.
Nicolas, A. and J.P. Poirier (1976) Crystalline plasticity and solid-state flow in metamorphic rocks, John Wiley.
Nimmo, F. (2004) What is the Young's modulus of ice? In *Workshop on Europa's Icy Shell,* Abstract #7005. Lunar and Planetary Institute, Houston.
Nimmo, F., and Pappalardo, R.T. (2016), Ocean worlds in the outer solar system, *J. Geophys. Res. Planets*, 121, 1378– 1399, doi:10.1002/2016JE005081.
Ottino, J. M., and D.V. Khakhar (2000), Mixing and Segregation of Granular Materials, *Annual Review of Fluid Mechanics*, *32*(1), 55-91, 10.1146/annurev.fluid.32.1.55.

Palguta, J., Schubert, G., and Travis, B. J. (2010) Fluid flow and chemical alteration in carbonaceous chondrite parent bodies. Earth and Planetary Science Letters, 296, 235–243.

Parmentier, E.M. and J.W. Head (1981) Viscous relaxation of impact craters on ice planetary surfaces, Icarus 47, doi: 10.1016/0019-1035(81)90095-6.

Parsons, B. and J.G. Sclater (1977) An analysis of the variation of ocean floor bathymetry and heat flow with age, J. Geophys. Res. 82, 803-827.

Postberg, F., S. Kempf J.K. Hillier, R. Srama, S.F. Green, N. McBride, E. Grün (2008) The E ring in the vicinity of Enceladus. II. Probing the moon's interior- th composition of E-ring particles, Icarus 193, doi:10.1016/j.icarus.2007.09.001.

Randolph-Flagg, N.G., T. Mittal, D. Hemingway (2020) Tidal pumping and heating of Enceladus' porous core, AGU Ocean Sciences Mtg, Abstract MG24A-2197.

Randolph-Flagg, N.G., (submitted 2023) Geophys. Res. Lett.

Reston, T.J. and C.R. Ranero (2011) The 3-D geometry of detachment faulting at mid-ocean ridges, GCubed 12, doi:10.1029/2011GC003666.

Roberts, J.H. (2015) The fluffy core of Enceladus, Icarus 258, doi:10.1016/j.icarus.2015.05.033.

Salaree, A. and E.A. Okal (2020) Effects of bathymetry complexity on tsunami propagation: a spherical harmonics approach, Geophys. J. Intl. 223, doi: 10.1093/gji/ggaa334.

Sandwell, D.T. and W.H.F. Smith, E Garcia, R Francis (2014) New global marine gravity model from CryoSat-2 and Jason-1 reveals buried tectonic structure, Science 346, doi:10.1126/science.1258213.

Schubert, G., J.D. Anderson, T. Spohn, W.B. McKinnon (2004) Interior composition, structure and dynamics of the Galilean satellites, in F Bagenal, TE Dowling, WB McKinnon (eds) Jupiter. The planet, satellites, and magnetosphere, p281-306, Cambridge Univ. Press.

Schwarzenbach, E.M. (2016) Serpentinization and the formation of fluid pathways, Geology 44, doi: 10.1130/focus022016.1.

Sclater, J.G., C. Jaupart, and D. Galson (1980), The heat flow through oceanic and continental crust and the heat loss of the earth, *Rev. Geophys. Space Phys.*, *18*, 269-311.

Showman, A.P., L. Han, W.B. Hubbard (2013) The effect of an asymmetric core on convection in Enceladus' ice shell: Implications for south polar tectonics and heat flux, Geophys. Res. Lett. 40, doi: 10.1002/2013GL057149.

Smith, D.K. and T.H. Jordan, Seamount statistics in the Pacific Ocean, JGR 93, doi: 10.1029/JB093iB04p02899.

Soderlund, K.M. (2019) Ocean dynamics of outer solar system satellites, GRL 46, doi:10.1029/2018GL081880.

Sotin, C., G. Tobie, J. Wahr, W.B. McKinnon (2009) Tides and tidal heating on Europa, in Europa, RT Pappalardo, WB McKinnon, KK Khurana (eds.) Univ. AZ Press p 85-118.

Sotin, C., K. Kalousova, G. Tobi (2021) Titan's interior structure and dynamics after the Cassini-Huygens mission, Ann. Rev. Earth. Planet. Sci. 49, 579-607, doi: 10.1146/annurev-earth-072920- 052847

Spinelli, G.A., E.R. Giambalvo, A.T. Fisher (2004) Sediment permeability, distribution, and influence on fluxes in oceanic basement, in Hydrogeology of the oceanic lithosphere EE Davis and H Elderfield (eds.) Cambridge Univ. Press, p 151.

Stein, C.A., and S. Stein (1992) A model for the global variation in ocean depth and heat flow with lithospheric age, Nature 359, 123-129.

Thomas, P.J. and G. Schubert (1986) Crater relaxation as a probe of Europa's interior, J. Geophys. Res. 91, 453-459.

Tolstoy, M., F. Waldhauser, D.R. Bohnenstiehl, R.T. Weekly, W-Y. Kim (2008) Seismic identification of along-axis hydrothermal flow on the East Pacific Rise, Nature 451, doi: 10.1038/nature06424.

Tontoni, F.C., T.J. Crone, C.E.J. deRonde, D.J. Fornari, J.C. Kinsey, E. Mittelstaedt, M. Tivey (2016) Crustal magnetization and the subseafloor structure of the ASHES vent field, Axial Seamount, Juan de Fuca Ridge: implications for the investigation of hydrothermal sites, GRL 43, doi:10.1002/2016GL069430.

Travis, B.J., J. Paguta, G. Schubert (2012) A whole-moon thermal history model of Europa: impact of hydrothermal circulation and salt transport, Icarus 218, doi: 10.1016/j.icarus.2012.02.008.

Turcotte, D. and G Schubert (1982) Geodynamics: Applications of continuum physics to geological problems, John Wiley & Sons, NY.

Villinger, H., I. Grevemeyer, N. Kaul J. Hauschild, M. Pfender (2002) Hydrothermal heat flux through aged oceanic crust: where does the heat escape? EPSL 202, 159-170, doi: 10.1016/S0012-821X(02)00759-8.

Waite, J. H. et al. Cassini finds molecular hydrogen in the Enceladus plume: evidence for hydrothermal processes. *Science* 356, 155–159 (2017).

Wheat, C. G., M. J. Mottl, A. T. Fisher, D. Kadko, E. E. Davis, and E. Baker (2004), Heat and fluid flow through a basaltic outcrop on a ridge flank, *Geochem. Geophys. Geosystems*, *5*(12), doi:10.1029/2004GC000700.
Wheat, C. G., and A. T. Fisher (2008) Massive, low-temperature hydrothermal flow from a basaltic outcrop on 23 Ma seafloor of the Cocos Plate: Chemical constraints and implications, *Geochemistry, Geophysics, Geosystems*, 7: doi:10.1029/2008GC002136.
Winslow, D.M. and A.T. Fisher (2015) Sustainability and dynamics of outcrop-to-outcrop hydrothermal circulation, Nat. Comm 6, doi: 10.1038/ncomms8567.
Winslow, D.M., A.T. Fisher, P.H. Stauffer, C.W. Gable, G.A. Zyvoloski (2016) three-dimensional modeling of outcrop-to-outcrop hydrothermal circulation on the eastern flank of the Juan de Fuca Ridge, J. Geophys. Res. 121, doi:10.1002/2015JB012606.
Wood, D.M (1998) Life cycles of granular materials, Phil. Trans. RAS 356, 2453-2470.
Zahnle, K., P. Schenk, H. Levison, L. Dones (2003) Cratering rates in the outer solar system, Icarus 163, doi:10.1016/S0019-1035(03)00048-4.